

## Noise Reduction in CMOS Image Sensors for High Quality Imaging: The Autocorrelation Function Filter on Burst Image Sequences

Kazuhiro Hoshino<sup>1</sup>, Frank Nielsen<sup>2,3</sup>, Toshihiro Nishimura<sup>4</sup>

<sup>1</sup>*Image Sensor Business Group, Sony Corporation,*

4-14-1 Asahi-chou, Atsugi-shi, Kanagawa, Japan

Kazuhiro.Hoshino@jp.sony.com,

<sup>2</sup>*Sony Computer Science Laboratories, Inc.*

3-14-13 Higashi Gotanda, Shinagawa-ku, Tokyo, Japan

Frank.Nielsen@acm.org

<sup>3</sup>*École Polytechnique, LIX, F-91128 Palaiseau Cedex, France*

<sup>4</sup>*Graduate School of Information, Production and Systems, Waseda University*

2-7 Hibikino, Wakamatsu, Kitakyushu, Fukuoka, Japan

toshi-hiro@waseda.jp

### Abstract

We propose a new method for image noise detection and reduction in complementary metal oxide semiconductor (CMOS) image sensors inspired from audio noise cancelling techniques. Our algorithm is based on computing efficiently the time-dependent pixel autocorrelation function (ACF) from constant time interval acquired sequences of images. We demonstrate the effectiveness of our approach for successfully detecting and reducing white noise. Further, we consider an adaptive filter that exhibits significant computational improvements making it highly practical. Finally, we report on experiments displaying the high-quality imaging systems obtained in practice.

**Keywords:** CMOS image sensor, white noise, autocorrelation function (ACF), noise canceller.

### 1 Introduction

Digital still and video cameras equipped with CMOS image sensors are well-known to be prone to noise phenomena, especially in poor lighting dim environments [20, 7, 18, 4, 3, 9]. It is therefore of the utmost importance to consider image processing noise reduction techniques to circumvent these sensor limitations in order to deliver crispy and vivid artefact-free images to consumers.

Typically, the various sources of noise in a CMOS image sensor can be classified into two disjoint groups: Namely, the *white noise* (W), and the *colored noise* (C). Noise sources occur either at the pixel circuitry level or in the analog-to-digital converter (ADC) unit.

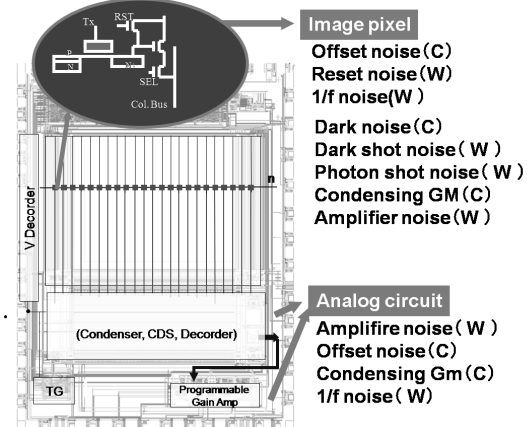


Figure 1: Source and classification of the two types of noise in a CMOS image sensor. The ‘W’ and ‘C’ attributes respectively mean white and colored noises.

White noise sources include the reset,  $1/f$ , dark shot, photon shot and amplifier noise, just to name a few. Colored noise include the offset noise, the dark noise, and the difference of dimension, among others. Figure 1 depicts these various types of noise along with their physical origin locations and White/Colored type classifications.

Colored noise is a *fixed pattern* noise that does not change over time as the images are read out. In other words, colored noise is time invariant, and depend only on the physical structural properties of the camera imaging system. For example, colored noise may originate from the threshold value or size scatter of a transistor, or from the sensitivity scattering and open



area ratio of a photo diode, or also from the gain scattering of the amplifier units, etc. It is well-known that such a kind of colored noise may be removed by applying the technique called *correlated double sampling* (or CDS for short), as described in [15]. Thus the system noise taking place in a camera device is colored and originates from the architecture *per se*. In principle, colored noise can be analyzed and ideally removed by subtracting to the captured image data the optimal (noisy) “black” data image obtained at the *same time* when no light hit the sensor. To contrast with these system-specific colored noise sources, the second class of noise, called white noises, have characteristics depending on *time* (and therefore is different in each acquired image). White noise sources include thermal, reset,  $1/f$  and optical noise (see Figure 1). Since the white noise does not have a constant (colored) signature, the simple former CDS filtering technique cannot fully reduce it. Thus it is of the crucial importance to remove as much as possible white noises in CMOS image sensors for high quality imaging. This well-known problem is further observed and delicate to tackle in dim environments.

Most of the white noise generated in CMOS image sensor are thermal noise that statistically follows a normal distribution (Gaussian distribution with the bell shape), so that a mean filter is effective for reducing its presence. However, the mean filter acts as a band passing filter and will degrade the signals by blurring image details such as natural edges. Although by averaging several frames we can significantly reduce noise<sup>1</sup>, its amount cannot be quantified nor tracked using this technique.

In this paper, we introduce an adaptive filter method for measuring and attenuating white noise at the pixel level. That is, we perform at each pixel a time-serie analysis based on the autocorrelation function (ACF) for detecting and quantifying the amount of white noise individually. This paper is based on seminal results that were first presented at the 2007 International Symposium on Industrial Electronics meeting (ISIE, see [6]).

The remainder of the paper is organized as follows: Section (2) presents the autocorrelation function framework and its use for detecting white noise in CMOS image sensors by exhibiting the analogy with audio noise-cancelling technique. Section (3) reports on our experimental settings for evaluating image quality of our filter algorithm. It is followed by Section (4) presenting our noise reduction results and the extended adaptive filter making use of prescribed thresholds derived from experiments. Finally, Section (5) concludes this paper.

<sup>1</sup>Formally proved by considering that each frame is statistically modeled as independent and identically distributed (iid.) sets of pixels, and applying the central limit theorem on each pixel value sequence.

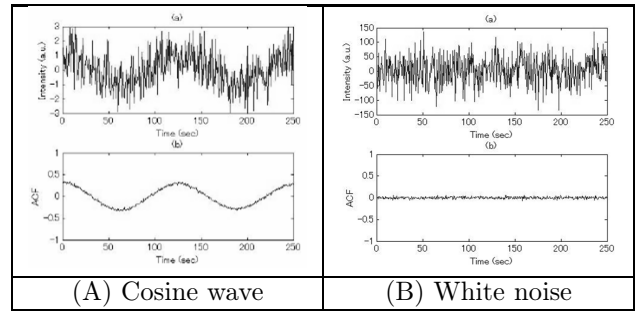


Figure 2: Wave signals and corresponding autocorrelation functions for (A) a cosine wave and (B) a random white noise .

## 2 Overview of our method

### 2.1 ACF for image processing

#### 2.1.1 Fourier analysis and the ACF

Consider a univariate *mixed* signal that consists of a 1D source signal *corrupted* with a white noise signal. The mixed signal is said noisy, and the goal of signal analysis is to recover the pure source signal from the corrupted signal. One of the key methods of signal processing is the autocorrelation function (ACF) that provably works only for periodic signals, see [1, 5, 10, 13, 16, 12, 14]. ACF is used for extracting from a noisy signal the source signal using Fourier analysis. We recall here concisely its basic principles. The Fourier spectrum of a function  $g(x)$  is given by

$$G(f) = \int_{-\infty}^{\infty} g(x) \exp(-2\pi ixf) dx, \quad (1)$$

where  $f$  denote the variable in frequency/phase domain (as opposed to the dual source – spatial – domain  $x$ ), and  $i$  represents the imaginary complex number  $i^2 = -1$ . The power spectrum  $\phi(f)$  is obtained as the complex modulus of  $G(f)$ , that is:

$$\phi(f) = |G(f)|^2 = G(f) \times G^*(f), \quad (2)$$

where  $*$  denotes the conjugate operator in the complex plane  $\mathbb{C}^2$ . The Fourier transform of Equation 1 is purposely rewritten as

$$\phi(\tau) = \int_{-\infty}^{\infty} \phi(f) \exp(-2\pi ixf\tau) df. \quad (3)$$

It follows from Eq. 1 and Eq. 2 that Eq. 3 yields

$$\phi(\tau) = \int_{-\infty}^{\infty} g(x)g(x + \tau) dx. \quad (4)$$

Eq. 4 is precisely the autocorrelation function of  $G(f)$ .

#### 2.1.2 Noise cancelling

In digital audio where signals are discretized into binary strings (the time-serie audio bit streams), the



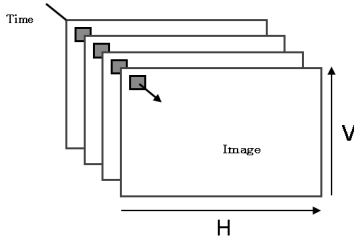


Figure 3: The auto-correlation function (ACF) considers the profile of the pixel intensity values from a sequence of images acquired at constant time interval.

discrete equivalent of the former integral ACF is used for noise cancelling. More precisely, we compute the following discrete summand

$$R(\tau) = \frac{1}{N} \sum_{t=0}^{N-\tau-1} x(t+\tau)x(t), \quad (5)$$

where  $N$  denotes the sampling size,  $x$  the *normalized* signal value in  $[-1, 1]$ ,  $t$  the time, and  $\tau$  the time shift. The ACF value  $R(\tau)$  ranges within the normalized bounded interval  $[-1, 1]$ .

### 2.1.3 Pixel ACF

In this work, we consider the former discrete audio ACF framework for performing *image* noise reduction by applying the ACF noise cancelling technique to each pixel individually. Thus in our novel setting, each pixel may be interpreted as an independent source of 1D signal (by analogy to audio signals), and  $N = w \times h$  denote the total number of pixels,  $t$  the horizontal coordinates,  $\tau$  the shifted pixel number of Eq. 5. That is, in order to detect the white noise using the ACF, we shift pixel horizontally<sup>2</sup> and perform auto-correlation. Note that in natural 2D images, correlations between neighbor pixels abound in textural areas while they tend to disappear at edge proximity.

As mentioned earlier, there are limitations of the ACF technique for detecting white noise: we need periodic signals. Indeed, Figure 2(A) displays the ACF plots for both a cosine and a random wave. Figure 2(A) shows the effectiveness of the ACF approach for removing white noise from a periodic signal. Consider now Figure 2(B) that plots the ACF for a white noise source signal. In this case, the ACF value slightly oscillates around zero ( $ACF \simeq 0$ ), and therefore fails to detect the presence of white noise.

This intrinsic limitation motivates our study of the time-axis ACF described next.

<sup>2</sup>Any other direction is possible. We chose arbitrarily the horizontal direction for ease of presentation.

## 2.2 Time-axis ACF for white noise detection

We perform the ACF for each pixel value on the *time axis* for detecting white noise by reinterpreting Eq. 5 as follows:

$$R(\tau) = \frac{1}{N} \sum_{t=0}^{N-\tau-1} x(t+\tau)x(t), \quad (6)$$

with now  $N$  denoting the sampling size,  $x$  the normalized signal value,  $t$  time, and  $\tau$  the time shift. That is, we consider for each physical pixel a corresponding 1D signal induced by an *image sequence*. Figure 3 graphically depicts the time-axis ACF for a given pixel in a sequence of images taken at constant interval. Such an image burst acquisition mode is becoming commonplace in digital still cameras where the bottleneck is saving the stream of pictures rather than reading them out of the image sensors. The ACF is computed independently for each pixel following the arrow in the illustration of Figure 3.

For static scenes, where pixel values remain unchanged in all acquired frames, the ACF always yield 1. However, since in practice the pixel value slightly fluctuates at each frame by some amount of white noise, it follows that the ACF is not perfectly 1 but oscillates a bit around this peak. Now notice that for a pixel imaging a dark area, the impact of white noise becomes important and the ACF fluctuates much more (later on described in terms of signal-to-noise ratio).

Thus the originality of our contribution is to study empirically the quantity of white noise estimated by the time-dependent ACF values, and derive from that analysis an efficient adaptive filter based upon. The next section briefly sketches our experimental setting. We then report on our experimental findings.

Table 1: Summary of our experimental setting.

|                   |   |                         |
|-------------------|---|-------------------------|
| Image sensor type | : | CMOS image sensor       |
| Image resolution  | : | 2.0 million pixels      |
| Capture interval  | : | 1/5 second              |
| #captured images  | : | 50 pictures             |
| Exposure time     | : | 1/20 second             |
| White balance     | : | Fixed                   |
| Gain              | : | Fixed                   |
| ISO               | : | 1600                    |
| F number          | : | 3.5                     |
| Data format       | : | Native 12-bit raw       |
| Converted format  | : | 24-bit RGB bitmap (BMP) |



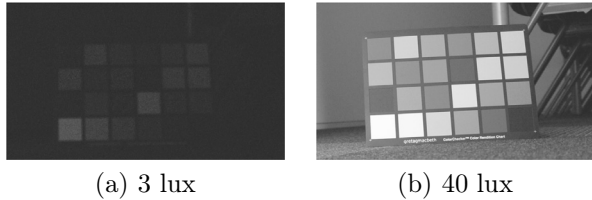


Figure 4: Acquiring a Gretag Macbeth colorplate image sequence under different illumination conditions (3 and 40 lux, respectively). Only the first image of the sequence is shown in (a) and (b). Observe that (a) exhibits different noise characteristics than (b).

### 3 Experimental setting

Table 1 summarizes the characteristics of the CMOS camera system used for carrying the evaluation experiments. The sensor image size is about 2.0 million pixels and 50 images were acquired at regular time interval: namely, burst mode at 1/5 second per frame. The exposure time was set to 1/20 second and the iris F-number controlling by the aperture size was set to 3.5 (incoming amount of light). The sensitivity index standardized by the International Standard Organization<sup>3</sup> was set to 1600 ISO. We captured the Gretag Macbeth color chart as displayed in Figure 4 both under low and normal illumination conditions, for analysis and comparisons. The low illuminance scene was shot at about 3 lux, and was primarily acquired for studying the effect of the ACF in the case where the white noise becomes significant compared to the source signal. This explains why photographers avoid that situation by using flashes. All images were saved in 12-bit native raw format and were also later post-processed and converted into standard 8-bit RGB bitmap images (24-bit truecolor tone-mapped bitmaps).

## 4 Result analysis of the ACF filter

### 4.1 ACF values of pixels

Figure 5 plots the ACF value as a function of the frame number in the image sequence for the case of a “bright” pixel labeled A (intensity 180 on 256 pixel value steps). This bright pixel A shows experimentally almost constant ACF value around the maximum 1.00 (precision up to two digits, ie.,  $10^{-2}$ ). We conclude that, in this case, that a large amount of light entered the photo diode and therefore the signal-to-noise ratio (SNR) is large, and as a matter of fact the impact of white noise is not significant in such a bright environment. On the contrary, in the case of a “dark” pixel labeled B in Figure 5, the SNR has a smaller value

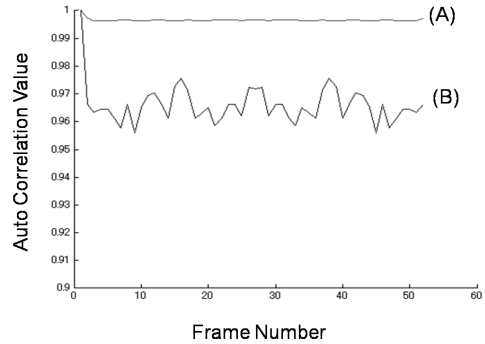


Figure 5: Plotting the time-dependent ACF value as a function of the frame number for two different normalized intensity pixels: (A) bright pixel with intensity 180/256, and (B) dark pixel with intensity value 8/256. Observe that the fluctuation amplitudes are correlated to the SNR value.

and therefore the contribution of the white noise in the mixed signal cannot anymore be ignored. We observe that the amount of white noise is correlated to the fluctuations of the time-dependent ACF, as depicted in the plots of Figure 5. This key observation is at the core of our proposed filter that we described next.

### 4.2 Noise reduction algorithm

In practice, since it is too time-consuming in imaging systems to compute the ACF for all pixels, we designed a filtering methodology summarized in the flow-chart diagram of Figure 6. In order to reduce the computational complexity, we set two thresholding tests with prescribed values as follows: First, only the pixel values that have their intensity values under a prescribed threshold are extracted. We choose  $I_{\text{threshold}} = 10$  for our current camera system, but this threshold should be set according to the selected image sensor and camera system. Our experimental study of the ACF depicted in Figure 5 suggests that indeed “bright” pixel with high SNR do not suffer much from white noise. For pixel intensity values below the prescribed threshold, the time-axis ACF is computed from the burst image sequence and a second ACF threshold test is performed to detect whether that value is below 0.8 or not, as indicated in the flow-chart of Figure 6. On one hand, for pixel whose ACF value falls below this 0.8 threshold, the filter tags the pixel as significantly deteriorated by white noise, and an auxiliary *noise correction* procedure is called upon to recover the proper denoised pixel value. On the other hand, for pixels ACF values above the threshold, the amount of white noise is considered neglectable and the pixel intensity values are left unchanged, even for pixels imaging dark areas. Observe that this filter can be run in parallel for all image pixels at once. Another possibility would be to extract

<sup>3</sup><http://www.iso.org>



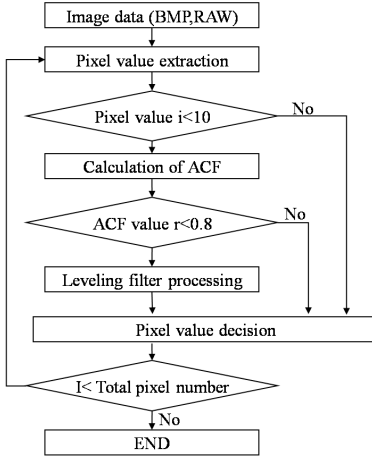


Figure 6: Synopsis of our proposed two-stage filter algorithm that reduces overall calculation cost.

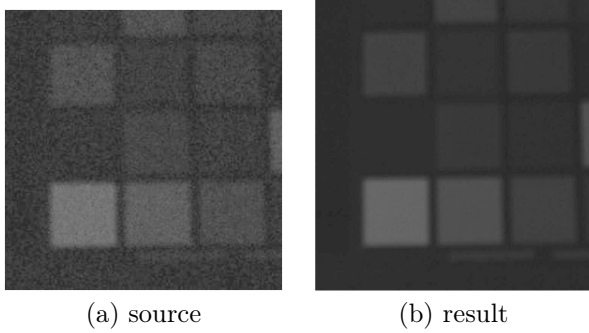


Figure 7: Asserting the ACF filter performance: (a) source image, and (b) ACF noise-reduction filtered image.

a bunch of low-level ACF pixels and perform the denoising processing on them at once.

Figure 7 shows the result of this algorithm on the former low illumination color-chart Gretag Macbeth picture (captured at 3 lux). We subjectively confirm that the level of noise was significantly decreased by this ACF adaptive filter algorithm. Note that since the filter is not called for bright pixels (above intensity 10), the resolution of the image is preserved in those areas while the amount of noise is minimized in dim areas.

Table 2: Experiment setting.

|                             |   |                    |
|-----------------------------|---|--------------------|
| Picture size                | : | $1936 \times 1296$ |
| F value                     | : | 3.5                |
| Exposure time               | : | 1/250 second       |
| ISO                         | : | 500                |
| #pictures                   | : | 20                 |
| Time shift between pictures | : | 1/5 second         |



(a) Source



(b)  $I \leq 100$



(c)  $I \leq 100$   
 $ACF \leq 0.995$

Figure 8: Filter performance: (a) source image, and (b) and (c) noise-reduction threshold mask images.

#### 4.3 Filter response under various brightness conditions

In order to evaluate furthermore the performance of the ACF filter algorithm, we carried out a serie of experiments in an office room that exhibit both dark and bright areas, as shown in Figure 8. The camera-system and shooting condition setting of our experiments are summarized in Table 2. Figure 8 shows the acquired picture: Namely, the first picture of a burt sequence of twenty shots. In Figure 8(b), only the pixels with intensity values under 100 are shown while the others are masked. These unmasked pixels account for 53% of the source image. After performing the ACF noise reduction filter, we display in Figure 8(c) the pixels with ACF value smaller than 0.995. These pixels represent 22% of the image.

In order to tune the threshold values required by our ACF noise reduction filter, we further investigated the computational complexity of applying the filter as a function of the ACF threshold value for a given natural image. Figure 10 displays a close-up of the picture shown in Figure 8(a) of the actual processing carried out for various ACF threshold values: 0.985, 0.995 and 1.0, respectively. This study allows one to *subjectively* evaluate the image quality and permits us to choose the appropriate trade-off computation time ( $\sim$  overall number of selected pixels)/image quality. For example, a change in image quality is hardly perceived with the ACF threshold value 0.985 of Figure 10(b) compared with the original source pic-



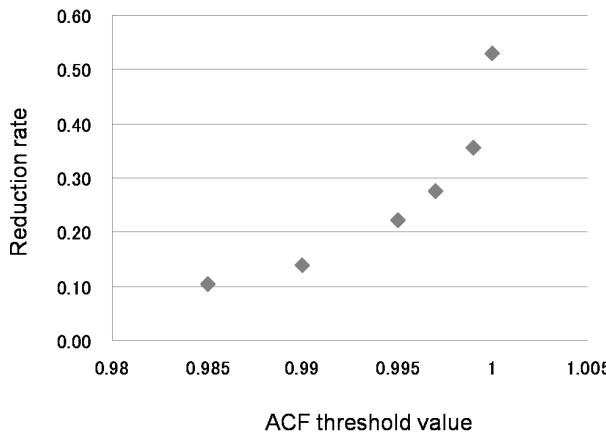


Figure 9: Evaluation of the overall filter time complexity as a function of the ACF value.

ture Figure 10(a). However, for the ACF value threshold set to 0.995 of Figure 10(c), we notice that the noise is removed in dark portions such as the strut portion of the chair shown in these close-up pictures. Figure 10(d) displays the noise-reduction technique performed for all pixels with intensity values below the prescribed threshold by setting the ACF threshold value to its maximum value 1.0. In that case, although the image quality is best, the problem becomes its computational tractability as indicated by the exponential curve of Figure 9.

We observe from that serie of experiments that the image quality is not degraded at the pixel boundaries where the ACF filter response change. That is, after careful inspection of the filtered image, we could not find any trace of edge halation phenomena. Edge halation is characterized by the spreading of light beyond its proper boundaries, and could have potentially be a side-effect of our ACF filter that processes image pixel islands. However, we confirmed in practice that this phenomenon does not occur, and that the ACF filter enhances drastically image quality, especially in poor lighting environments.

## 5 Conclusion

In this paper, we proposed a novel approach for performing noise-reduction in CMOS camera systems inspired by audio signal processing. Our new filter is based on the autocorrelation function (ACF) that finds its root in Fourier analysis. The ACF filter processes in parallel independently all image pixels by computing the time-axis ACF from burst image sequences, and by deciding from the respective ACF values the set of pixels containing a fair amount of white noise that need to be adjusted. Since it is quite computationally intensive to perform that processing operation for all pixels, we designed a two-level indirection branching algorithm that allows to

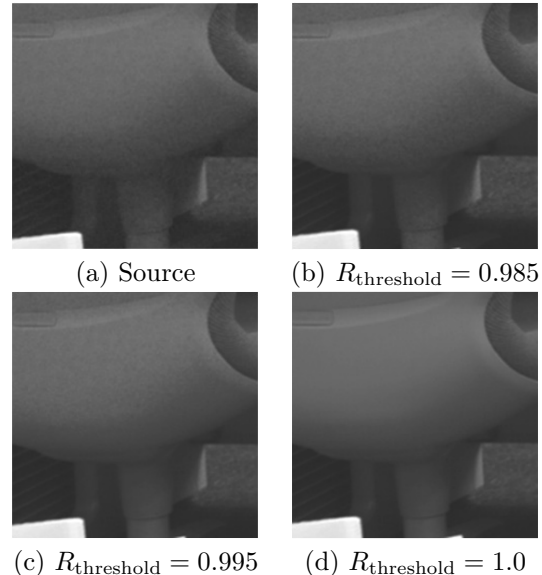


Figure 10: Comparisons of image quality for various ACF threshold values. (a) source image, and (b), (c), and (d) filter performance when setting the pixel value threshold at  $I_{\text{threshold}} = 100$  (see synopsis of Fig. 6) for various threshold values  $R_{\text{threshold}} \in \{0.985, 0.995, 1.0\}$  of the ACF.

significantly reduce the number of selected pixels by thresholding both on the pixel intensity and on the ACF values. By carrying out a serie of experiments, we demonstrated that our algorithm is well-suited for high quality imaging systems as it effectively attenuates the amount of white noise in images, especially in low lighting challenging environments. A careful inspection further shows that there were no image quality discontinuities nor edge halation phenomena introduced as a side-effect by this adaptive ACF filter. Our study let us conclude that the time-axis ACF adaptive filter yields an effective solution for dealing with detection and correction of white noise in CMOS camera systems, and contribute to high quality imaging systems.

## Acknowledgements

We would like to acknowledge the technical support of Mr. Shinohara and Nakagawa of the University of Waseda, Japan.

## References

- [1] S. Akaho, *Scale and rotation invariant features based on higher-order autocorrelations*, Bulletin of the Electro Technical Laboratory, vol. 57, no. 10, pp. 973-981, 1993.

- [2] S. Akaho, *The EM algorithm for multiple object recognition*, IEEE International Conference on Neural Networks (ICNN), pp. 2426-2431, 1995.
- [3] H. Belahrach, M. Karim, and J. Farre, *Noise characterization in CMOS APS imagers for highly integrated imaging systems*, 13th International Conference on Microelectronics, pp. 31-34, 2003.
- [4] J. E. Carnes and W. F. Kosonocky, *Noise sources in charge coupled devices*, RCA Rev., vol. 33, pp. 327-343, 1972.
- [5] F. Goudail, E. Lange, T. Iwamoto, K. Kyuma, and N. Otsu, *Face recognition system using local autocorrelations and multiscale integration*, IEEE Transactions on Pattern Analysis and Machine Intelligence, vol. 18, no. 10, pp. 1024-1028, 1996.
- [6] K. Hoshino, H. Sumi, and T. Nishimura, *Noise detection and reduction for image sensor by time domain autocorrelation function method*, IEEE Proceedings of International Symposium on Information and Computer Elements (ISICE), pp. 1737-1740, 2007.
- [7] J. Hynecek, *Analysis of the photosite reset in FGA image sensors*, IEEE Transactions on Electron Devices, vol. 37. No. 10. pp. 2193-2200. 1990.
- [8] T. Ihara, T. Nagai, K. Ozeki, and A. Kurematsu, *Noise Reduction in Time Domain Using Referential Reconstruction*, IEICE Transactions on Information and Systems, vol. E89-D, pp. 1203-1213, 2006.
- [9] C. Jung, M. H. Izadi, L. Michelle. L. Haye G. H. Chapman, and K. S. Karim, *Noise analysis of fault tolerant active pixel sensors*, IEEE International Symposium on Defect and Fault Tolerance in VLSI Systems, 2005.
- [10] M. Kreuts, B. Volpel and H. Jansen, *Scale-invariant image recognition based on higher-order autocorrelation features*, Pattern Recognition, vol. 29, no. 1, pp. 19-26, 1996.
- [11] S. Kodama, M. Nakamura, H. Kitao, and O. Iwata, *Effect of pre-processing of high-pass filter in speech detection using short-time auto-correlation*, IEICE technical report, vol. 103, no. 398, pp. 37-42, 2003.
- [12] N. Kunieda, *A study on noise level estimation utilizing autocorrelation function*, IEICE technical report, vol. 103, no. 633, pp. 49-54, 2003.
- [13] T. Masuda and N. Yokoya, *A robust method for registration and segmentation of multiple range images*, Computer Vision and Image Understanding, vol. 61, no. 3, pp. 295-307, 1995.
- [14] N. Nakagawa, K. Hoshino, and T. Nishimura, *A method of 1/f noise characteristic extraction on image sensor by using auto correlation function*, IEICE technical report, ME and Bio Cybernetics, vol. 106, no. 506, pp. 45-48, 2007.
- [15] R. H. Nixon, S. E. Kemeny, C. O. Staller, and E. R. Fossum, *256 × 256 CMOS active pixel sensor camera on a chip*, IEEE Journal on Solid State Circuits, 31(12), pp. 2046-2050, 1996.
- [16] N. Otsu, *A threshold selection method from gray-level histograms*, IEEE Transactions on System, Man, and Cybernetics, vol. SMC-9, no. 1, pp. 62-66, 1979.
- [17] H. Tian and A. El Gamal, *Analysis of temporal noise in CMOS photodiode active pixel sensor*, IEEE Transactions on Circuits and Systems-II, Analog and Digital Signal Processing, vol. 48, No. 2, 2001.
- [18] N. Teranishi and N. Mutoh, *Partition noise in CCD signal detection*, IEEE Transactions on Electron Device, ED-33, pp. 1696-1701, 1986.
- [19] M. H. White, D. R. Lanpe, F. C. Blaha, and I. A. Mack, *Characterization of surface channel CCD image arrays at low light levels*, IEEE Journal on Solid State Circuits, SC-9, pp. 1-13, 1974.
- [20] K. Yonemoto and H. Sumi, *A CMOS image sensor with a simple fixed pattern noise reduction technology and a hole accumulation diode*, IEEE Journal Solid-State Circuits, vol. 35, issue 12, pp. 2038-2043, 2000.





**Kazuhiro Hoshino** is a researcher in imaging technology. He obtained the Bachelor Science degree from Yokohama National University in 1984. He started research of LSI process in 1998 and joined in 1999 the international microelectronics center (IMEC) in Belgium as a researcher in advanced LSI processing and later in CCD image sensors. His research interests are camera systems, CMOS image sensors and noise reduction. He is with Sony Corporation and he preparing his Ph. D. in Waseda University, Japan.



**Frank Nielsen** defended his PhD thesis on adaptive computational geometry prepared at INRIA Sophia-Antipolis (France). In 1997, he served in the army as a scientific member in the computer science laboratory of Ecole Polytechnique. In 1998, he joined Sony Computer Science Laboratories Inc., Tokyo (Japan), where he is senior researcher. His current research interests include geometry, vision, graphics, learning, and optimization. He authored the book *Visual Computing: Geometry, Graphics, and Vision*, ISBN 1584504277, 2005.



**Toshihiro Nishimura** is an associate professor of Waseda University. He is interested in neural network, neuron science, healing science, CMOS image sensor, power electronics, medical imaging, visual cognitive science, hearing cognitive science, brain science and artificial vision. He is currently affiliated with the Information Architecture, Graduate School of Waseda University, Japan.

